



ECONOMIC GEOLOGY
RESEARCH UNIT

University of the Witwatersrand
Johannesburg

MAJOR ADDITION OF MAGMA AT
THE PYROXENITE MARKER IN THE
WESTERN BUSHVELD COMPLEX,
SOUTH AFRICA

R. GRANT CAWTHORN, PETER S. MEYER
AND F. JOHAN KRUGER

• INFORMATION CIRCULAR No. 235

UNIVERSITY OF THE WITWATERSRAND
JOHANNESBURG

MAJOR ADDITION OF MAGMA AT THE PYROXENITE MARKER IN THE WESTERN
BUSHVELD COMPLEX, SOUTH AFRICA

by

R. GRANT CAWTHORN¹, PETER S. MEYER² and F. JOHAN KRUGER³

¹ Department of Geology, University of the Witwatersrand, P.O. Wits
2050, South Africa

² Department of Geology, Woods Hole Oceanographic Institution,
Woods Hole, Massachusetts, 02543, U.S.A.

³ Bernard Price Institute for Geophysical Research, University of the
Witwatersrand, P.O. Wits 2050, South Africa)

ECONOMIC GEOLOGY RESEARCH UNIT
INFORMATION CIRCULAR No. 235

May, 1991

MAJOR ADDITION OF MAGMA AT THE PYROXENITE MARKER IN THE WESTERN
BUSHVELD COMPLEX, SOUTH AFRICA

ABSTRACT

A major, but gradual, reversal in the cryptic variation pattern of the plagioclase and pyroxenes, of 13 mole % anorthite and 10 mole % Mg/(Mg+Fe) respectively, is documented in the Main Zone of the western Bushveld Complex. These changes are accompanied by a decrease in initial $^{87}\text{Sr}/^{86}\text{Sr}$ ratio from greater than 0.708 to less than 0.707. The Pyroxenite Marker, a distinctive orthopyroxenite layer, occurs close to the top of this reversed differentiation sequence. This is attributed to addition of less differentiated magma. On the basis of a mass balance calculation of the initial $^{87}\text{Sr}/^{86}\text{Sr}$ ratios, it is estimated that the volume of magma added was comparable to that of the resident magma.

Increases in the Fe_2O_3 , TiO_2 , Al_2O_3 and Na_2O contents of the pyroxenes above the level of magma addition indicate that the new magma had a lower silica activity and higher $f\text{O}_2$ than the resident magma. Quantification of the trace and REE content of the two magmas is hampered by the very low proportion of trapped intercumulus component in these adcumulate rocks. However, semi-quantitative modelling indicates that the trace and REE signatures of the two magmas were similar, with moderate LREE enrichment and flat HREE profiles. The new magma had a slightly higher La/Sr ratio than the resident magma, consistent with its more alkaline nature.

The new magma was probably added gradually, while 100–150m of cumulates formed. It probably intruded at an intermediate level within an existing stratified magma chamber, where it cooled and crystallized, and composite packets of liquid plus crystals plunged to the base of the chamber. The cores of plagioclase grains formed during this mixing interval show a wider range of compositions than in other sections and plagioclase primocrysts from both magmas may be preserved within single samples. Therefore, while intimate physical mixing of packets of unknown size of the two magmas occurred, re-equilibration of the major oxide composition of the plagioclase primocrysts was not achieved. However, the data and calculations based on diffusion rates indicate that partial Sr isotopic resetting of plagioclase may have occurred.

—oo—

MAJOR ADDITION OF MAGMA AT THE PYROXENITE MARKER IN THE WESTERN

BUSHVELD COMPLEX, SOUTH AFRICA

CONTENTS

	<i>Page</i>
INTRODUCTION	1
GEOLOGY	2
PETROGRAPHY	2
MINERAL COMPOSITIONS	4
WHOLE-ROCK CHEMISTRY	10
DISCUSSION	12
Differences in Magma Compositions	12
Relative Volumes of Magmas	14
Incompatible Trace Element Content of the Magmas	15
Magma Addition and Mixing at the Pyroxenite Marker	21
Postcumulus Processes	22
Pyroxenite Marker	23
SUMMARY	25
ACNOWLEDGEMENTS	25
REFERENCES	25

_____oo_____

Published by the Economic Geology Research Unit
Department of Geology
University of the Witwatersrand
1 Jan Smuts Avenue, Johannesburg 2001
South Africa

ISBN 1 874856 26 5

MAJOR ADDITION OF MAGMA AT THE PYROXENITE MARKER IN THE WESTERN
BUSHVELD COMPLEX, SOUTH AFRICA

INTRODUCTION

The mafic rocks of the Bushveld Complex can be divided into four zones, Lower, Critical, Main, and Upper, and reach a maximum thickness of 8 km. Pyroxenites predominate in the Lower Zone, whereas orthopyroxene, plagioclase and chromite assemblages comprise the Critical Zone. The Main Zone is regarded as more homogeneous or monotonous, being dominated by noritic to gabbroic rocks, although isotopically it is very heterogeneous (Hamilton, 1977; Sharpe, 1985). The Upper Zone consists of gabbro, anorthosite, and magnetitite layers with the appearance of olivine and apatite towards the top of the sequence. The review by Wager & Brown (1968) excellently summarises the mineralogy and petrography of these rocks. The plagioclase and pyroxene compositions reported by them and Atkins (1969) did not reveal any major reversals, possibly due to the wide sample spacing especially in the Main Zone. However, more detailed studies by Von Gruenewaldt (1973) and Molyneux (1974) documented a reversal in mineral compositions, as well as a reversal from inverted pigeonite to primary orthopyroxene in the Main Zone, which provide evidence for the addition of less differentiated magma. Within this zone or reversed differentiation they identified a thin layer of orthopyroxenite which they termed the Pyroxenite Marker, and traced over considerable distances around the eastern Bushveld Complex. This horizon has not been recognised in the western Bushveld Complex, but Walraven & Wolmarans (1979) reported a reversal in the plagioclase compositions in a section through the Main Zone indicating that magma addition had also occurred in this sector of the Bushveld Complex. Subsequent studies have shown that a sustained change in initial $^{87}\text{Sr}/^{86}\text{Sr}$ ratio occurs at this horizon (Sharpe, 1985; Kruger *et al.*, 1987), consistent with the concept of magma addition. It is for this reason that Kruger *et al.* (1987) place the boundary between the Main and Upper Zones at this horizon.

At present, much research is focussed on the fluid dynamic processes associated with magma addition and the mixing or stratification of magmas (Sparks *et al.*, 1984; Turner & Campbell, 1986, Campbell & Turner, 1989), and the exact composition of the different magmas which produced the Bushveld Complex (Cawthorn *et al.*, 1981; Sharpe, 1981; Irvine *et al.*, 1983). However, until more precise estimates of magma compositions are available it is difficult to predict the relative temperatures, densities and viscosities of the various magmas, which are the fundamental physical parameters in fluid dynamic modelling.

The rocks are almost pure accumulates (Cawthorn & Walsh, 1988) and the major element chemistry reflects the cumulus mineralogy, and offers only indirect information about parental magma compositions. Nevertheless, some information on certain characteristics of the different magmas can be gleaned from incompatible trace element and isotopic data as demonstrated by Hamilton (1977), Cawthorn (1983) and Kruger *et al.* (1987). This study is an attempt to provide geochemical constraints on the nature and interaction of the two magmas involved in the formation of the rock sequence straddling the Pyroxenite Marker in the western Bushveld Complex. Cumulus mineral compositions, strontium isotopic ratios and REE and incompatible trace element abundances have been determined in order to investigate magma compositions and evaluate the mixing processes involved.

GEOLOGY

The extent of outcrop in the western Bushveld Complex is shown in Figure 1. Exposure is generally very poor, but the lithological sequence has been determined by Coertze (1970). The entire succession is preserved in the centrally dipping arc from Pretoria to Thabazimbi, whereas only the lower portion is preserved in a shallow synclinal body to the west of the Pilanesberg Complex.

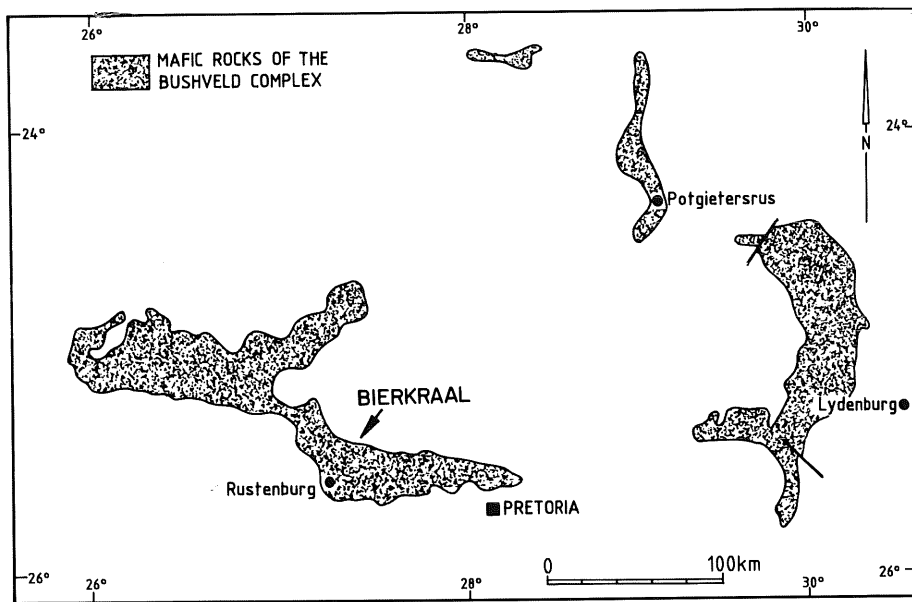


Figure 1: Simplified geological map showing the extent of the mafic rocks of the Bushveld Complex. The location of the farm Bierkraal where the boreholes were located is indicated (Walraven and Wolmarans, 1979). A composite stratigraphy of all boreholes is given in Kruger *et al.* (1987).

The Geological Survey of South Africa drilled three stratigraphic boreholes near Bierkraal (Fig. 1) through the Upper Zone and the upper half of the Main Zone. The stratigraphy and major lithological units have been reported by Kruger *et al.* (1987). Borehole BK2 was sited near the base of the magnetite-bearing Upper Zone, intersected the Pyroxenite Marker at 484 m and penetrated some 600 m of the underlying Main Zone. The typical dip of the layering in this region is 24° to the north (Walraven and Wolmarans, 1979). All depths quoted in this paper refer to depths in the vertical borehole core, and so distances between samples are approximately 9% greater than their true stratigraphic separation.

PETROGRAPHY

Fifty one samples spanning 1000 m of the BK2 succession have been studied. The depths at which samples were taken are given in Table 2 and were selected to be representative of the typical lithological and textural rock types. Their modal proportions are shown in Figure 2. Typically 20 cm of core (diameter 5 cm) was cut in half lengthwise. A small piece was broken off for petrographic

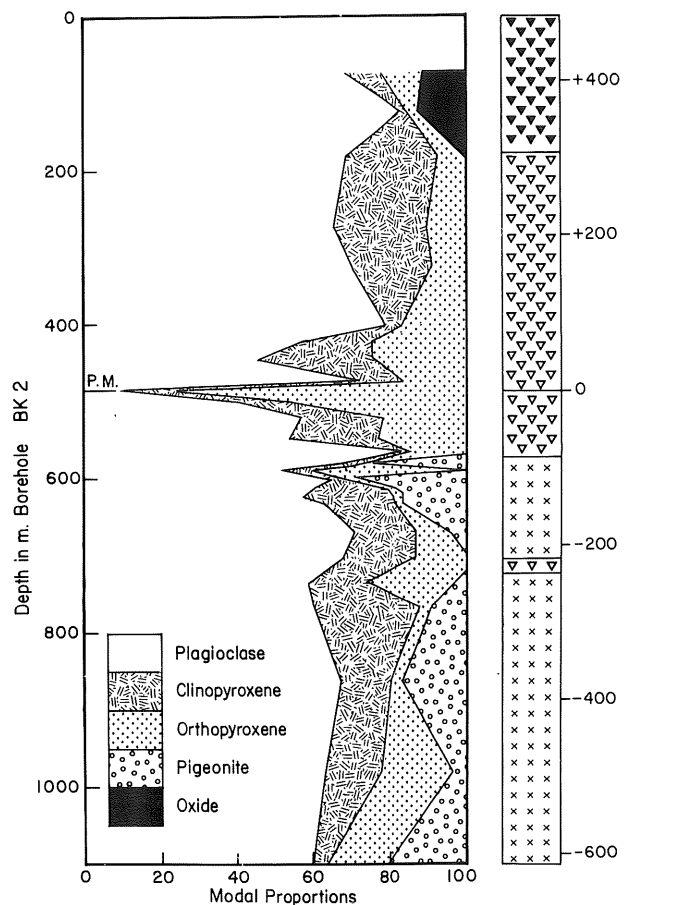


Figure 2: Plot of modal proportions of 51 samples from borehole BK2. Depths in borehole at which samples were studied are given in Table 2. Depths have not been corrected for dip which is approximately 24° to the north-northeast (Walraven & Wolmarans, 1979). P.M. indicates position of the Pyroxenite Marker. The simplified lithological log on the right hand side indicates depths in metres relative to the Pyroxenite Marker and shows inverted pigeonite gabbro, orthopyroxene gabbro and magnetite orthopyroxene gabbro as crosses, open triangles, and solid triangles, respectively, and is included on all subsequent figures. Note that the horizon at which inverted pigeonite disappears is 5m below the Pyroxenite Marker, whereas both are coincident in the eastern Bushveld (Von Gruenewaldt, 1973).

and electron microprobe analysis, the remainder of the half core being crushed for chemical analysis. The rocks of the succession are dominated by gabbronorite accumulates, essentially devoid of any other minerals except pyroxene and plagioclase. However, due to the overgrowth on cumulus grains and mutual interference between crystals the grains are rarely perfectly euhedral. A few of the samples from 600 to 100 m below the Pyroxenite Marker contain extremely sparse interstitial magnetite and biotite. The uppermost three samples contain abundant magnetite.

The Pyroxenite Marker occurs at a depth of 484 m in the borehole and is 65 cm thick, with a sharp lower and gradational upper contact, and contains idiomorphic orthopyroxene with anhedral clinopyroxene and plagioclase. It is very similar to the Pyroxenite Marker which occurs in the eastern sector (Von Gruenewaldt, 1973). The base of this apparently ubiquitous and distinctive layer was used as the reference datum for the profile in this study. In the tables and text depths are quoted relative to this horizon; negative distances referring to samples below the Pyroxenite Marker, positive numbers above it. On all diagrams both the depth in the borehole and the distance relative to the Pyroxenite Marker are given for reference.

There was a complex relationship involving the crystallization of primary orthopyroxene and pigeonite. The original primary pigeonite has inverted during slow cooling to produce the orthorhombic paramorph with abundant exsolution lamellae of calcic clinopyroxene. To distinguish between this and the primary orthopyroxene which contains little exsolution, the paramorphic form will be referred to henceforth as inverted pigeonite to indicate that the magmatic mineral had the high temperature monoclinic symmetry. These two types of pyroxene are indicated separately in Figure 2.

MINERAL COMPOSITIONS

Plagioclase, primary orthopyroxene, and Ca-rich clinopyroxene were analysed for major and minor elements (Table 1) using the JEOL JXA-50A electron microprobe at the University of Rhode Island. Analyses were carried out with a focussed beam and counting times of 30 seconds or until 60,000 counts were collected. For the plagioclase grains, several analyses of the cores and rims were determined on each of several grains. The cores of different grains show a significant range in composition, as shown in Figure 3, sometimes by as much as 12 mole % An. However, the average core compositions show a definite trend. From a depth of 601 to 188 m below the Pyroxenite Marker a normal differentiation trend is observed from An₆₇ to An₅₈. The 200 m section above this displays a wider scatter of core compositions but the average becomes more calcic, reaching An₇₄ 36 m above the Pyroxenite Marker. Above this, a normal differentiation trend is resumed up to the top of the profile, where the composition is An₅₅ and the range of core compositions is more restricted.

Walraven & Wolmarans (1979) reported the compositions of plagioclase from a surface traverse between Bierkraal and Rustenberg, and they documented the existence of a significant reversal in composition of the cores, comparable to that reported here.

The plagioclase rim compositions show a wide range of values, which can largely be attributed to the timing at which mutual interference between adjacent grains terminated further growth. Normal zonation is most common, although it rarely exceeds 5 mole % An. However, both normal and reverse zoning is observed in samples immediately below the Pyroxenite Marker.

The total iron content (as Fe₂O₃ in weight percent) in the core of the plagioclase is given in Table 1. At the base of the profile it ranges from 0.09 - 0.21 %. In the section above 117 m below the Pyroxenite Marker values range from 0.33 to 0.48 %. The uppermost sample, which contains magnetite, shows a low Fe₂O₃ content in the plagioclase of 0.20%. The range of K₂O concentrations in the plagioclase is from 0.18 to 0.32 %, but there is no correlation or systematic change as a function of height.

TABLE 1
Average mineral analyses

	Depth (m)	75	275	425	482	484	492	501	567	601	672	881	980	1095	
	Depth*	409	209	59	2	0	-8	-17	-83	-117	-188	-377	-496	-611	
<i>Clinopyroxene</i>															
SiO ₂	51.20	51.34	52.14	50.65	51.34	51.17	51.44	51.00	51.89	51.30	52.12	52.18	51.67	51.45	
TiO ₂	0.35	0.51	0.59	0.66	0.58	0.57	0.59	0.41	0.46	0.36	0.43	0.43	0.45	0.45	
Al ₂ O ₃	1.46	1.68	1.84	1.80	1.73	1.77	1.90	1.75	1.48	1.36	1.17	1.34	1.52	1.52	
Fe ₂ O ₃	1.89	2.23	2.13	3.30	2.71	2.43	2.40	1.71	1.85	1.45	1.79	1.21	1.79	1.79	
FeO	9.85	6.80	6.15	7.51	6.44	7.90	6.21	10.99	6.01	8.58	6.75	7.62	7.56	7.56	
MnO	0.36	0.31	0.28	0.18	0.18	0.16	0.30	0.38	0.36	0.23	0.32	0.24	0.24	0.24	
MgO	13.12	14.31	15.54	14.48	14.38	14.68	14.67	14.41	15.68	13.98	15.10	15.11	15.19	15.19	
CaO	21.25	21.89	21.46	20.59	21.97	20.40	22.10	18.58	21.25	21.38	21.96	21.19	20.65	20.65	
Na ₂ O	0.21	0.32	0.29	0.28	0.31	0.29	0.34	0.26	0.27	0.19	0.22	0.19	0.19	0.19	
Cr ₂ O ₃	0.00	0.08	0.14	0.22	0.20	0.20	0.25	0.16	0.07	0.04	0.02	0.01	0.02	0.02	
Total	99.68	99.46	100.53	99.67	99.84	99.57	100.20	99.80	99.51	99.48	99.63	99.26	99.26	99.26	
<i>Orthopyroxene</i>															
SiO ₂	50.95	52.76	54.03	52.93	52.57	52.29	53.14	52.15	53.46	51.91	53.16	52.44	52.70	52.70	
TiO ₂	0.24	0.25	0.22	0.26	0.32	0.36	0.22	0.34	0.24	0.27	0.41	0.25	0.29	0.29	
Al ₂ O ₃	0.72	0.79	0.93	0.79	0.86	0.87	0.85	0.82	0.66	0.60	0.54	0.58	0.86	0.86	
Fe ₂ O ₃	0.64	0.76	0.96	1.26	0.71	2.26	0.79	0.55	0.52	0.43	0.38	0.43	0.77	0.77	
FeO	26.85	20.55	17.01	20.22	20.59	19.74	19.74	22.74	18.46	23.41	20.85	20.18	18.93	18.93	
MnO	0.75	0.58	0.49	0.36	0.39	0.36	0.57	0.56	0.57	0.65	0.57	0.60	0.51	0.51	
MgO	18.54	23.44	25.88	23.27	22.98	23.01	24.05	21.52	25.19	21.37	23.64	24.18	24.18	24.18	
CaO	1.39	1.52	1.66	1.15	0.98	1.26	1.17	1.61	0.95	1.34	0.95	1.02	1.43	1.43	
Na ₂ O	0.01	0.03	0.02	0.01	0.00	0.04	0.02	0.03	0.01	0.02	0.01	0.02	0.01	0.01	
Cr ₂ O ₃	0.04	0.04	0.06	0.16	0.08	0.11	0.14	0.12	0.06	0.03	0.03	0.01	0.03	0.03	
Total	100.11	100.73	101.26	100.41	99.48	100.30	100.68	100.42	100.11	100.04	100.23	99.70	99.68	99.68	
<i>Plagioclase</i>															
SiO ₂	54.23	51.97	50.21	50.75	51.67	51.09	49.98	51.24	51.06	53.31	52.75	52.25	50.29	50.29	
Al ₂ O ₃	28.62	30.48	31.16	30.83	30.25	30.59	31.37	30.31	30.63	29.08	29.47	31.03	29.54	31.03	
Fe ₂ O ₃	0.19	0.48	0.36	0.41	0.44	0.44	0.34	0.29	0.10	0.18	0.08	0.19	0.08	0.08	
CaO	11.39	13.32	14.56	14.35	13.74	14.25	14.61	13.62	13.83	11.85	12.38	12.74	14.27	14.27	
Na ₂ O	4.97	3.83	3.20	3.30	3.56	3.38	3.18	3.68	3.57	4.60	4.32	4.15	3.24	3.24	
K ₂ O	0.23	0.25	0.20	0.29	0.26	0.17	0.19	0.21	0.32	0.21	0.21	0.30	0.19	0.19	
Total	99.63	100.34	99.69	99.93	99.92	99.92	99.67	99.34	99.39	99.22	99.17	99.11	99.11	99.11	

* Numbers refer to depth in metres in borehole relative to the Pyroxenite Marker.

Pyroxene averages are of 7-11 analyses. Only core compositions are averaged for plagioclase.

The trend for the pyroxene compositions has strong similarities with that for the plagioclase. The mole % En for the orthopyroxene is shown in Figure 3. The range of compositions for any one sample is fairly small, usually less than 3 mole % En. From the base of the section up to 188 m below the Pyroxenite Marker there is a normal differentiation trend. As with the plagioclase there is a significant reversal of 9 mole % En at -117 m. Above this there is an overall reversed trend to +59 m, whereafter normal differentiation resumes.

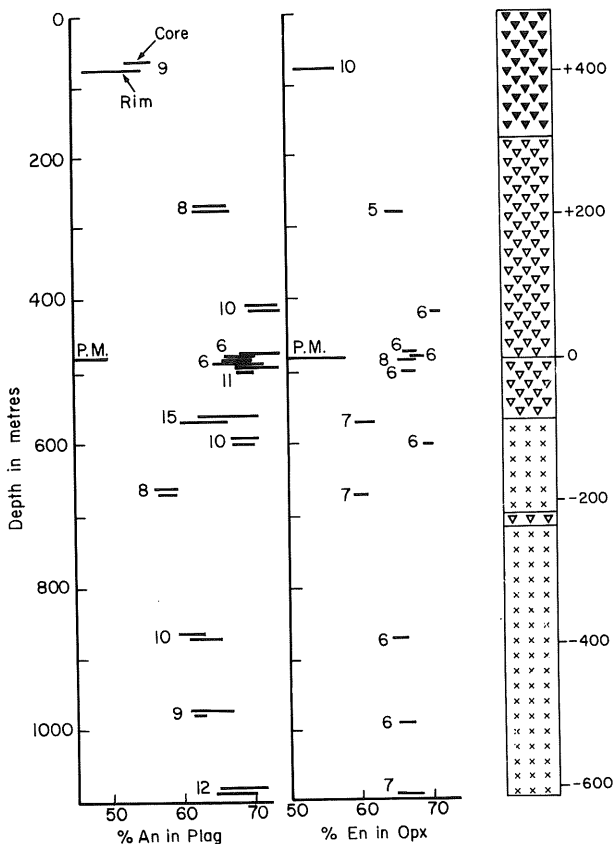


Figure 3: Plot of depth in borehole BK2 versus composition of plagioclase and orthopyroxene. The number of grains analysed is indicated and the range of compositions of cores and rims of the plagioclase is shown by the upper and lower lines, respectively, in each pair. For the orthopyroxene there is very little difference between the core and rim of individual grains. The Mg/(Mg+Fe) ratio for the clinopyroxenes is not shown, but parallels the orthopyroxene trend.

The Mg/(Mg+Fe) ratio for the calcium-rich clinopyroxene compositions parallels the trend for the orthopyroxene (Table 1), and so is not included in Figure 3. The sample from -83 m appears to be anomalous as it has a lower Ca content than all the other clinopyroxenes. This sample has only 2.5% modal clinopyroxene, usually as small interstitial grains, and the analyses show a wide range of Ca contents. The KD $\text{K}_{\text{D}}(\text{Mg}/\text{Fe})$ $\text{K}_{\text{D}}(\text{Mg}/\text{Fe})_{\text{opx}}$ for this sample is 1.38 whereas all other samples give values between 1.66 and 1.94. The low K_{D} and low Ca content in the

clinopyroxene for this sample suggest higher blocking temperatures. The plagioclase also shows a far greater range of core compositions than other samples. The reason for these anomalies is not known.

Based on the average analyses in Table 1, and using the recalculation scheme of Lindsley (1983), the clinopyroxenes show a range of blocking temperatures from 700-500°C. Such low temperatures are also suggested by the large K_D values discussed above. A significant range of Ca contents was recorded in both pyroxenes (2 % and 3 % Wo in the orthopyroxene and clinopyroxene respectively). Consequently, no more precise attempt has been made to determine equilibration temperatures. Lindsley (1983; Fig. 13) suggested that the coexistence of three pyroxenes could be used as a thermometer, which would record the magmatic rather than subsolidus re-equilibration temperature. The En value for the orthopyroxene in samples below the Pyroxenite Marker where three pyroxenes coexist is 66-70, giving a temperature of about 1150°C. Above the Pyroxenite Marker no inverted pigeonite was observed within the section studied even though higher in the succession the pyroxenes become more Fe-rich than below the Marker. This implies that the temperature for the transition from orthopyroxene to pigeonite must be lower in the magma above the Pyroxenite Marker, than below it. The transition from primary orthopyroxene to inverted pigeonite occurs within the magnetite-rich sequence of the Upper Zone.

The Fe_2O_3 content of the pyroxenes has been calculated assuming perfect stoichiometry (Cawthorn & Collerson, 1974). Concentrations for both pyroxenes are shown in Figure 4. The clinopyroxene always contains approximately three times the Fe_2O_3 content of the orthopyroxene. Values are relatively low for samples below -117 m, but from -117 to +59 m there is an increase by almost a factor of two. Above this height, Fe_2O_3 contents generally decrease, but remain higher than for samples below -117 m.

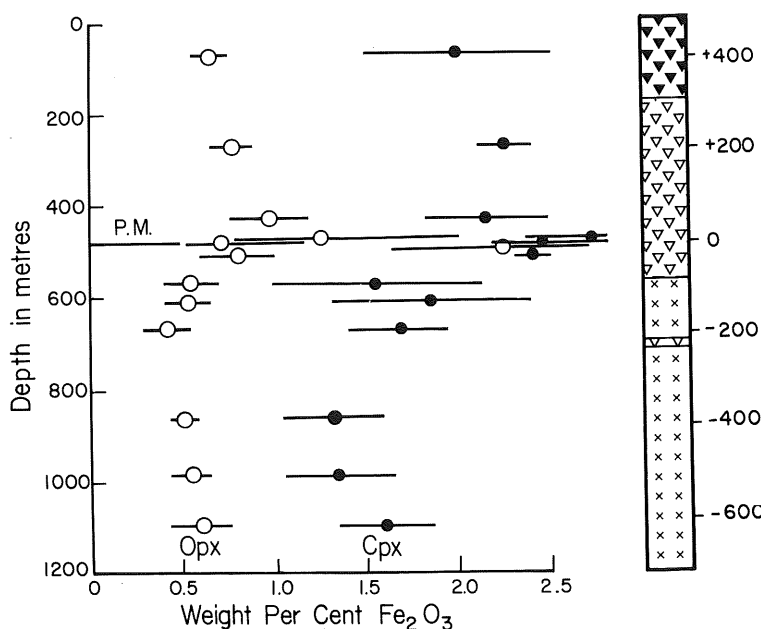


Figure 4: Plot of calculated Fe_2O_3 content of orthopyroxenes and clinopyroxenes assuming perfect stoichiometry versus depth in borehole BK2. Total range and average are indicated.

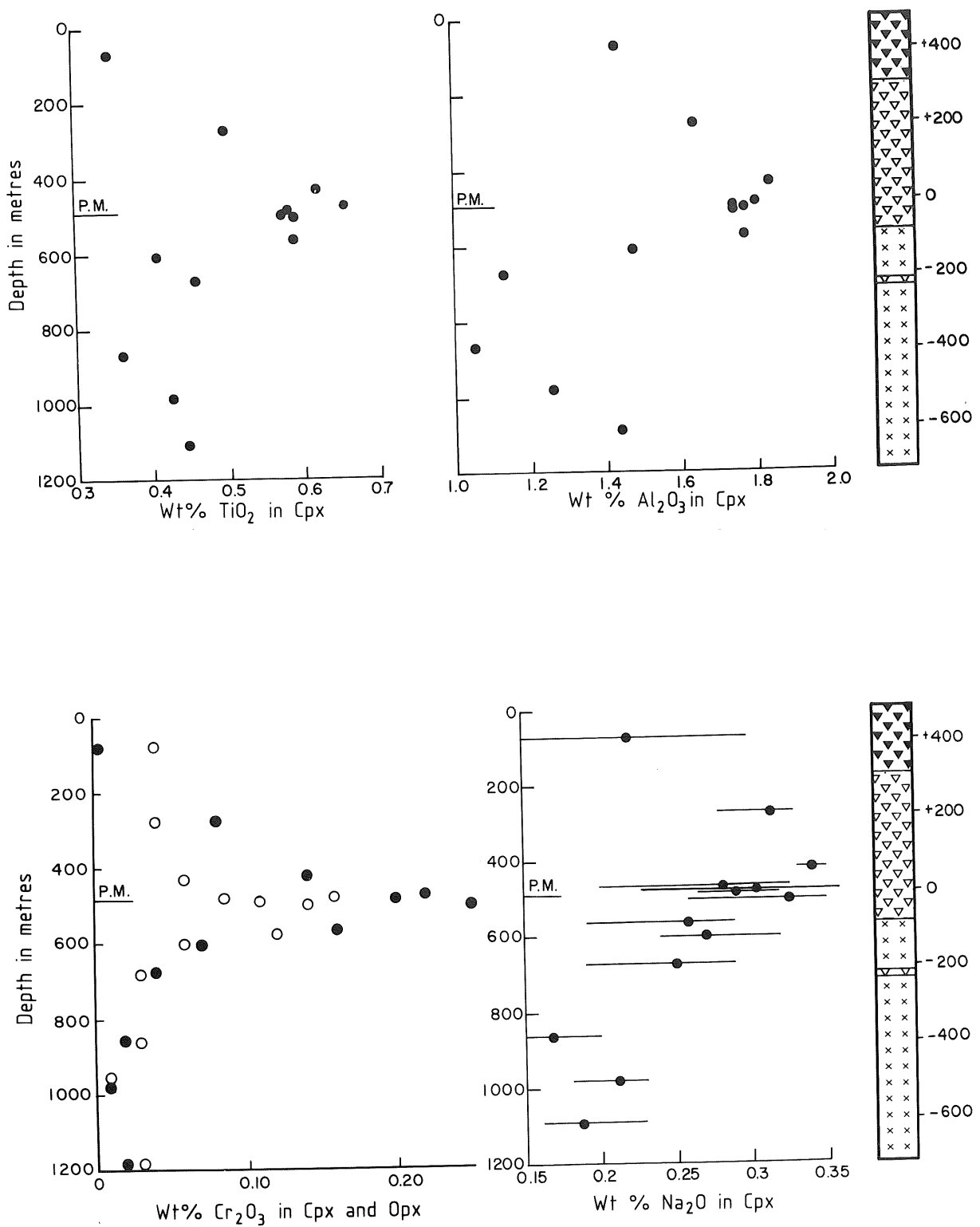


Figure 5: Plot of average TiO_2 , Al_2O_3 , and Na_2O contents in clinopyroxene, and Cr_2O_3 in orthopyroxene (open circles) and clinopyroxene (solid circles) versus depth in borehole BK2. Concentrations for other oxides in orthopyroxene are not included as they have lower abundances than clinopyroxene and do not show the break in trends as clearly (see Table 1). The total range of Na_2O values is indicated as a horizontal line as these show a particularly large variation.

Similar trends exist for the TiO_2 , Al_2O_3 , Cr_2O_3 and Na_2O contents of the clinopyroxene (Fig. 5). An increase in all values is

TABLE 2
Trace element abundances

<i>Depth (m)</i>	<i>Depth*</i>	<i>Rb</i>	<i>Sr</i>	<i>Y</i>	<i>Zr</i>	<i>P</i>	<i>Ba</i>	<i>K₂O</i>
75	409	9	287	9	34	102	160	0.37
124	360	4	395	7	34	41	185	0.36
182	302	3	283	14	34	115	98	0.26
225	259	5	253	14	41	86	110	0.27
275	209	5	279	11	32	90	102	0.26
324	160	2	280	9	25	15	74	0.21
375	109	7	267	12	34	124	126	0.28
402	82	3	285	10	29	61	108	0.19
425	59	3	216	16	29	1393	87	0.16
448	36	7	178	11	31	149	73	0.26
475	9	4	271	14	29	139	101	0.21
479.6	4.70	3	252	15	29		88	
481.9	2.40	3	228	11	23		81	
482.6	1.70	5	244	11	30		91	
483.6	0.70	2	228	11	24		74	
484.3	0	1	54	13	26	406	37	0.06
484.4	-0.10	4	116	13	27		37	
484.7	-0.40	28	358	7	31		116	
484.9	-0.50	2	215	9	22		57	
486.2	-1.90	2	199	12	34		93	
488.4	-4	3	192	12	28		92	
491.9	-8	5	288	10	29		83	
501.0	-17	5	197	12	29	120	71	0.18
504.8	-21	3	160	13	33		72	
505.7	-22	5	148	13	30		118	
506.3	-23	4	280	9	24		106	
511.2	-27	3	181	11	25		59	
513.0	-29	5	163	13	38		81	
522.0	-38	5	226	10	32	148	91	0.26
529.0	-45	5	224	13	34		92	
542.0	-56	5	266	10	31		80	
560.0	-76	4	270	13	29		131	
579.4	-95	3	302	7	22		89	
582.0	-98	2	294	7	22	45	70	0.19
584.7	-100	2	278	11	22		130	
588.0	-104	4	231	9	29		120	
591.6	-108	2	305	9	24		111	
601	-117	6	214	5	24	30	84	0.19
612	-128	1	282	9	21	18	57	0.16
631	-147	1	277		19	39	69	0.15
672.8	-189	3	299	9	29	95	111	0.29
701.8	-218	3	283	10	31	112		0.26
707.5	-224	5	280	13	33	67		0.28
712.9	-229	6	279	15	35	66		0.32
717.9	-234	9	297	12	36	178		0.35
764.3	-280	6	270	9	24	59		0.29
861.5	-378	3	271	8	22	26		0.21
932.2	-448	4	318	12	24	43		0.28
980.7	-497	3	272	9	26	24		0.25
1073.6	-590	5	277	8	27		165	
1095.9	-612	7	248	9	41	104	106	0.29

Concentrations in ppm, except for K_2O (%).

Depth is position in m in borehole BK2.

* Position relative to the Pyroxenite Marker.

apparent at -117 m. The TiO_2 and Al_2O_3 contents of the orthopyroxene are considerably lower than for the clinopyroxene and they do not show as convincing a break at -117 m (see Table 1). Despite the low concentrations and correspondingly large uncertainty the Cr_2O_3 content does increase above this level.

The plagioclase and clinopyroxene in the sample from the Pyroxenite Marker are texturally intercumulus. However, the plagioclase composition is only slightly more albitic and no more strongly zoned than the over- and underlying cumulus plagioclase compositions (Fig. 3). Similarly, the clinopyroxene is no more Fe-rich than adjacent samples (Table 1). Hence, this sample would be termed a heteradcumulate using the nomenclature of Wager *et al.* (1960), and does not contain a greater proportion of intercumulus component than other samples in this sequence.

WHOLE-ROCK CHEMISTRY

Samples of core weighing 0.5 kg were crushed and analysed for Ba, Rb, Sr, Zr, Y, P, and K using a Phillips 1410 XRF spectrometer. The method for analysis of P as a trace element using pressed powder briquettes is reported in Cawthorn & Walsh (1988).

Concentrations of REE in whole-rock powders were determined by instrumental neutron activation analysis using the reactor at the University of Rhode Island and the method described by Schilling & Ridley (1975). Because of the low REE abundances, typical of adcumulate rocks, samples were irradiated for 14 hours (double the normal irradiation time for basalts).

Strontium isotope analyses were carried out on a VG MM30 mass spectrometer after separation of Rb and Sr using standard cation exchange techniques as described in Eales *et al.* (1990). Blank values were ≤ 4 ng and ≤ 10 ng respectively, but were negligible with respect to the 200 mg sample aliquots. Nine spiked and unspiked runs of SRM-987 yielded a ratio of 0.71023 ± 4 (2 s.d.). Fourteen replicate analyses of a single sample resulted in a 1 s.d. error of 0.5% on the Rb/Sr ratio, and 0.01% on the $^{87}Sr/^{86}Sr$ ratio. Duplicate analysis on 8 samples resulted in an average error of 0.00008 in the initial ratio. A comparison of the Rb and Sr values determined by isotope dilution and by XRF shows good agreement, generally within 2 ppm (see Tables 2 and 4).

Phosphorus was a highly incompatible element in all the minerals crystallizing in the succession. Henderson (1968) quoted an analysis of 20 ppm in a plagioclase separate from the Bushveld Complex, which would give a value for the partition coefficient of less than 0.01. Hence, the concentration of P can be used to estimate the quantity of mesostasis (Cawthorn and Walsh, 1988).

The REE contents of the samples are presented in Table 3 and Figure 6. All, except one sample at +59 m, show a significant positive Eu anomaly, which is expected as all samples contain cumulus plagioclase. The sample from +59 m is anomalous compared to all other samples as it contains a very minor amount of euhedral apatite, and so has a P content an order of magnitude larger than other samples. As apatite concentrates the REE (Watson & Green, 1981) this sample has the highest REE abundances, as shown in Figure 6. Apatite has a negative Eu anomaly (Watson & Green, 1981) and so the combined effect of the apatite and plagioclase in the sample at

TABLE 3
Rare earth element abundances

Depth (m)	75	275	425	501	567	601	672	861	980	1095
Depth*	409	209	59	-17	-83	-117	-188	-378	-496	-611
La	3.43	4.01	6.44	3.48	2.94	1.54	3.91	1.84	3.14	4.51
Ce	7.60	8.58	15.38	7.77	6.34	3.27	8.19	4.01	6.76	8.70
Nd	4.36	4.00	8.28	4.35	2.56	1.81	3.61	2.20	3.40	4.25
Sm	1.09	1.02	1.90	1.09	0.60	0.30	0.88	0.65	0.93	0.89
Eu	0.67	0.49	0.62	0.56	0.85	0.26	0.64	0.50	0.59	0.61
Gd			2.43		0.69		1.17	0.96		
Tb	0.21	0.24	0.30	0.26	0.10	0.10	0.16	0.14	0.19	0.21
Dy	1.24		1.84			0.64	0.95		1.23	1.21
Yb	0.81	0.81	1.03	0.91	0.39	0.36	0.56	0.54	0.65	0.65
Lu	0.115	0.125	0.160	0.143	0.050	0.059	0.075	0.077	0.097	0.096

Concentrations in ppm.

Depth is the sample position in m in borehole BK2.

* Sample position relative to the Pyroxenite Marker.

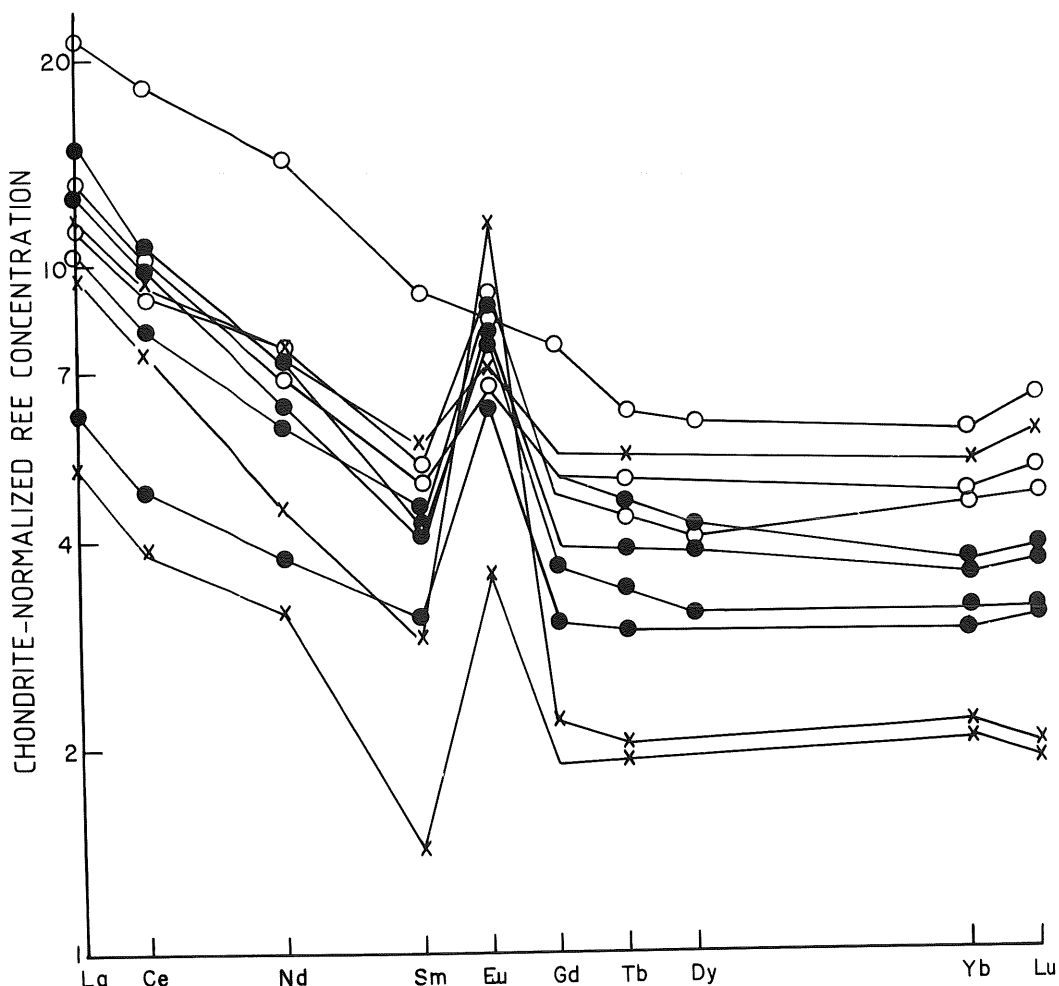


Figure 6: Chondrite-normalized REE content of cumulate rocks from borehole BK2. Open circles indicate samples from the Pyroxenite Marker and above; crosses indicate samples from immediately below the Pyroxenite Marker to a depth of -117m depth (the zone of magma addition and mixing); and solid circles represent samples from below -117m.

+59 m may have eliminated the Eu anomaly. The sample at -117 m apparently has a very low Sm value, but in other respects is similar to the other samples, suggesting that the analysis for Sm may be in error.

For the HREE (Gd-Lu) the three stratigraphic groups tend to have different absolute abundances (Fig. 6). The highest concentrations are found in the samples above the Pyroxenite Marker, while the transition zone from -117 m to the Pyroxenite Marker has the lowest abundances (with one exception). However, for the LREE this separation is not as clearly defined.

The extent of the positive Eu anomaly can be evaluated by calculating the theoretical value (Eu^*) by interpolating between Sm and Gd or Tb. The ratio Eu/Eu^* can be related to the proportion of plagioclase, as shown in Figure 7. For the two suites of samples above and below the Pyroxenite Marker there is a positive correlation between Eu/Eu^* and the proportion of plagioclase. The samples above the Marker have a systematically lower ratio for any plagioclase content than those below it. Above and below the Pyroxenite Marker the range of An contents in plagioclase is comparable, but the Eu/Eu^* ratios are different (Fig. 7), and hence the variation in Eu/Eu^* cannot be attributed to differences in plagioclase composition. With the exception of sample at -17 m there is no difference in the P content above and below the Pyroxenite Marker, and so differences in Eu/Eu^* cannot be related to varying proportions of apatite.

The range of Rb/Sr ratios for all the sample is so limited that an isochron plot is of little value. Instead, initial $^{87}\text{Sr}/^{86}\text{Sr}$ ratios have been calculated for all these samples (Table 4) using the preferred age of 2,060 Ma for the crystallization of the Bushveld Complex (Hamilton, 1977; Kruger *et al.*, 1987; Walraven *et al.*, 1990). In view of the very low Rb/Sr ratios, uncertainty in the age will not affect the initial ratio significantly. The initial ratios are plotted in Fig. 8. The lowest two samples show the same scatter as other published data on this part of the Main Zone (Hamilton, 1977; Sharpe, 1985; Kruger *et al.*, 1987). From -188 m to the Pyroxenite Marker there is a gradual decrease. There is then a rapid increase to a value of 0.7073 ± 1 (2 s.d.) which remains constant throughout the remainder of the Upper Zone (Kruger *et al.*, 1987).

DISCUSSION

Differences in Magma Compositions

Several lines of evidence suggest that the cumulates above the Pyroxenite Marker were not the differentiation products of the magma crystallizing below this horizon. The reversal in plagioclase and pyroxene composition and the change in Sr isotopic ratio are persuasive evidence of crystallization from different magmas. Furthermore, the change in the latter parameter implies that the new magma was fundamentally different from the resident magma, not merely less differentiated. The pyroxene compositions also show evidence for the two magmas being chemically distinct. Concentrations of minor elements in the pyroxenes show differences which cannot simply be related to varying degrees of differentiation. The Fe_2O_3 , TiO_2 , Al_2O_3 and Na_2O contents of the clinopyroxene (Fig. 5) show a marked increase above -117 m. The $\text{Mg}/(\text{Mg}+\text{Fe})$ ratios of the pyroxenes at -377m and +209m are comparable and so the

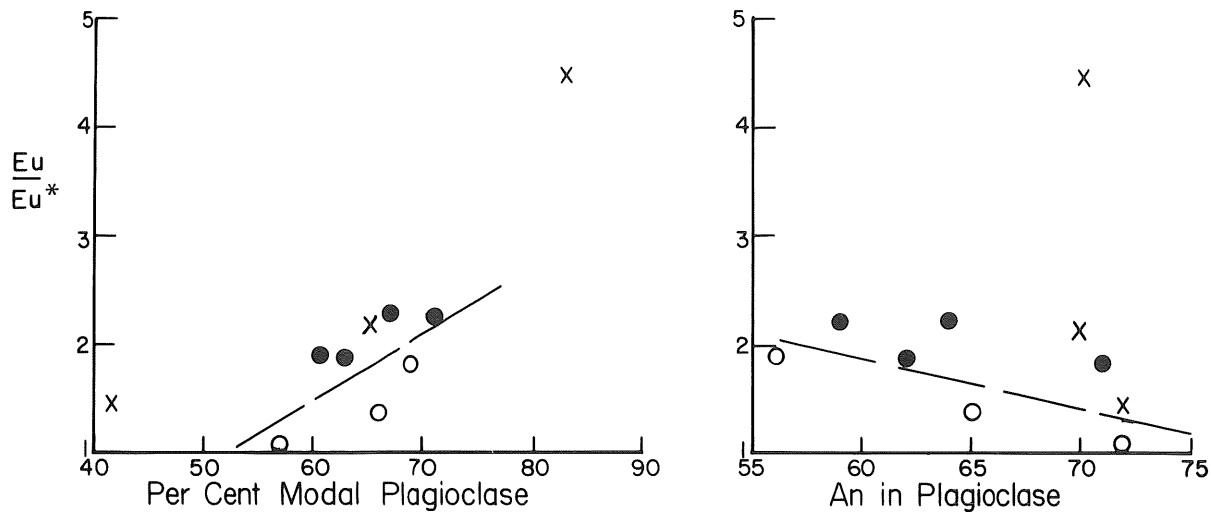


Figure 7: Plot of Eu/Eu^* as a function of proportion and core composition of plagioclase, demonstrating that the magnitude of the Eu anomaly increases with proportion of plagioclase as expected; and the anomaly does not depend on mineral composition. There is a smaller anomaly for samples above the Pyroxenite Marker (open circles), than below it. Symbols as for Figure 6.

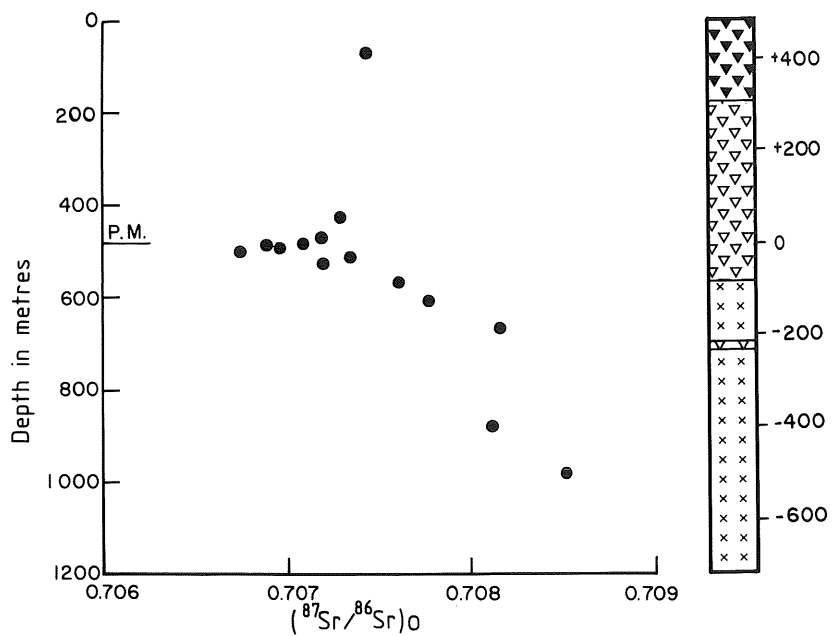


Figure 8: Plot of initial ${}^{87}\text{Sr}/{}^{86}\text{Sr}$ ratio versus depth in borehole BK2.

difference in abundance for these four elements is not due to the stage of differentiation of the magma. Clinopyroxenes crystallizing from magmas with a low silica activity have relatively high TiO_2 , Al_2O_3 , Fe_2O_3 and Na_2O contents (Coombs, 1963) and so the observed changes in these element abundances may reflect the addition of magma with a lower silica activity than that resident in the magma chamber. However, it was not so alkaline as to terminate the crystallization of orthopyroxene from the mixed magma.

Relative Volumes of Magmas

The Sr abundance and isotopic ratio may be used to estimate the relative proportion of new magma blended with resident magma. The initial $^{87}Sr/^{86}Sr$ ratio of the magma which formed the sequence of rocks from -607 to -188 m is 0.7082 (Table 4). The initial ratio of the completely mixed magma which forms the succession from +59 m to the top of the intrusion is 0.7073 (Table 4 and Kruger *et al.*, 1987). The isotopic ratio of the added magma prior to mixing is also required for the calculation. The lowest value obtained in this study is 0.7067, but it cannot be assumed that this does not include some component from mixing with the earlier magma. Davies & Cawthorn (1984) documented evidence for intrusion of magma into the lower part of the western Bushveld Complex, which they argued was representative of the magma added at the level of the Pyroxenite Marker. This magma had an initial ratio of 0.7063, and this is taken as the value for the new magma. This is consistent with the lowest value reported here of 0.7067 being due to slight contamination by the resident magma. However, in the southern lobe of the Bushveld Complex where less mixing has occurred, the Upper Zone has a lower ratio of 0.7055 (Kruger, unpublished data); but it has yet to be proved that this was identical to the magma which was intruded into the western lobe investigated here.

If it is assumed that the Sr contents of the two magmas were comparable, the isotopic ratios of the resident magma, the new magma, and the mixed magma indicate that the relative volume of new magma was approximately equal to that of the resident magma. As the total stratigraphic column above the Pyroxenite Marker is in excess of 2 km (Kruger *et al.*, 1987), this indicates that there must have been a major influx of magma at this horizon.

TABLE 4
Strontium isotopic data

Depth (m)	Depth* (m)	Rb	Sr	$^{87}Rb/^{86}Sr$	$^{87}Sr/^{86}Sr$	Initial ratio
75	409	7.67	266.7	0.0832	0.709912 ± 35	0.70744 ± 16
425	59	2.53	216.4	0.0338	0.708278 ± 30	0.70727 ± 14
475	9	3.71	272.4	0.0394	0.708360 ± 30	0.70719 ± 14
479.6	4	2.33	254.5	0.0265	0.707872 ± 4	0.70709 ± 14
484.3	0	0.98	49.8	0.0569	0.708599 ± 41	0.70691 ± 15
491.9	-8	4.72	292.5	0.0467	0.708352 ± 5	0.70697 ± 14
501	-17	2.69	191.3	0.0407	0.707962 ± 19	0.70675 ± 14
513	-29	4.35	162.3	0.0776	0.709650 ± 30	0.70735 ± 15
522	-38	4.88	225.4	0.0626	0.709056 ± 27	0.70720 ± 15
567	-83	1.73	338.7	0.0148	0.708034 ± 39	0.70760 ± 14
601	-117	5.37	211.3	0.0735	0.710003 ± 30	0.70782 ± 15
601 repl	-117		211.6		0.710021 ± 39	0.70784
672	-188	3.07	295.5	0.0301	0.709053 ± 27	0.70816 ± 14
672 repl	-188	3.08	296.9	0.0300	0.709102 ± 31	0.70821 ± 14
862	-378	1.73	278.9	0.0179	0.708646 ± 29	0.70811 ± 14
980	-496	2.74	267.8	0.0296	0.709380 ± 22	0.70850 ± 14

Depth is the sample position in BK2.

* Sample position relative to the Pyroxenite Marker.

Error on $^{87}Rb/^{86}Sr$ is 0.5% 1 S.D.

Error on $^{87}Sr/^{86}Sr$ is 0.01% 1 S.D. The precision shown here is 1 S.E. on ~100 ratios.

Initial ratio calculated using a decay constant of 1.42×10^{-11} , and age of 2060 ± 27 Ma. The 95% confidence limits take into account the errors in age, $^{87}Rb/^{86}Sr$, and $^{87}Sr/^{86}Sr$.

Incompatible Trace Element Content of the Magmas

In a cumulate rock the REE abundances are controlled by the proportion of cumulus phases, their partition coefficients and the proportion of intercumulus component. In a polyphase adcumulate rock it is almost impossible to petrographically estimate the intercumulus content. However, it is possible to use a geochemical technique, such as that discussed by Henderson (1975). The concentration of highly incompatible elements in the bulk rock gives a measure of the proportion of trapped liquid since it may be assumed that the elements are entirely concentrated in the intercumulus component. In this case, P is used as the incompatible element. The magma added at the level of the Pyroxenite Marker contained approximately 1000 ppm P (Davies & Tredoux, 1985). The samples immediately above the Pyroxenite Marker contain about 100 ppm P. Such a P content would be predicted for a rock with an intercumulus component of about 10 %. However, this new magma mixed with a resident magma which had undergone extensive fractional crystallization and hence probably had a significantly higher P content. Hence, 10% intercumulus component will be an upper value. Some of the samples below the Pyroxenite Marker contain less than 100 ppm P, so would have lower intercumulus content. For each sample an intercumulus content is determined using the P content of the rock and an assumed liquid content of 1,000 ppm. This ignores the effect of upwards enrichment due to fractionation of a magma of unknown P content, and the effect of mixing as both are difficult to quantify. However, it will be shown below that small errors in the absolute content of the intercumulus component do not greatly affect the calculated liquid compositions. Czamanske & Scheidle (1985) argued that the cumulates from the Banded Series of the Stillwater Complex contain no more than a few per cent of trapped liquid.

Using this geochemically estimated intercumulus content, the modal analysis of the rocks (converted to weight proportions) and the REE content of the sample, it is possible to calculate the REE composition of the magma from which each sample crystallized. The bulk composition of the rock is defined by the equation :

$$C_r = C_m (P_i \times D_i)$$

where :

C_r is the element concentration in the whole rock;

C_m is the element concentration in the magma;

P_i is the weight proportion of phase i present (including the intercumulus component), and

D_i is the partition coefficient for phase i (equal to unity for the intercumulus component).

The value for C_m is the only unknown in this equation.

The proportion of the intercumulus component as calculated here is analogous to the residual porosity of the cumulate as defined by Irvine (1982). Our model assumes that the crystals formed from the magma which finally solidified as the intercumulus component. In reality, there may have been vertical movement of interstitial magma as solidification progressed, but it is not possible to modify the calculations to accommodate this effect.

The partition coefficients used in these calculations are given in Table 5 and the calculated REE abundances for the magma are shown in Figure 9 and averages are given in Table 6.

TABLE 5
Mineral/liquid partition coefficients

	<i>Plag</i>	<i>Opx/Pig</i>	<i>Cpx</i>	<i>Apatite</i>
La	0.20	0.01	0.05	4.5
Ce	0.15	0.015	0.06	7.5
Nd	0.10	0.015	0.08	9.5
Sm	0.09	0.02	0.10	12.0
Eu	0.35	0.02	0.10	12.0
Gd	0.08	0.04	0.15	11.0
Tb	0.07	0.06	0.15	10.0
Dy	0.05	0.08	0.20	9.0
Yb	0.04	0.10	0.20	7.0
Lu	0.04	0.15	0.20	5.0

Values for silicates obtained from compilation of Irving (1978) using 1-atm experimental data.
Values for apatite from Watson & Green (1981) from hypersthene hawaiite composition.

TABLE 6
Chondrite-normalized concentrations of REE in magmas

	<i>Above 484 m</i>	<i>484–601 m</i>	<i>Below 601 m</i>	<i>New magma*</i>
La	67	47	52	82
Ce	58	42	44	72
Nd	48	37	37	59
Sm	31	23	26	36
Eu	23	26	26	
Gd	28	22	21	35
Tb	26	22	22	30
Dy	23	22	21	25
Yb	22	16	17	27
Lu	24	18	17	31
La/Lu	2.79	2.61	3.06	2.75
2Eu/(Sm + Gd)	0.75	1.16	1.11	
(Sm + Gd)/(Yb + Lu)	1.27	1.32	1.38	1.25

* Calculated assuming that the samples above 484 m represent crystallization from a magma derived by mixing equal proportions of resident magma represented by samples below 601 m and new magma.

Before these results can be discussed, it is necessary to establish the accuracy of the calculations. The major uncertainty is the P content of the magma, which is used to calculate the mesostasis content. To estimate the error which could be introduced in this way, a series of calculations have been performed for the sample at -188 m using a simplified mode of 60% plagioclase and 40 % pyroxene, and with 5, 10, 15 and 20% intercumulus component. The results are presented in Figure 10. It can be seen that increasing the intercumulus proportion by a factor of four has the effect of decreasing the absolute concentration of REE calculated for the magma by less than a factor of two, but it does not change the morphology of the REE profile except for the development of an Eu anomaly. The range from 5 to 20% trapped liquid far exceeds the uncertainty in the calculation of this component.

The calculated liquid profiles are shown in Figure 9. The samples from -612 to -188 m give calculated liquid compositions which define a coherent group showing slight LREE enrichment and an almost flat profile through the HREE. In one sample there is a very small positive Eu anomaly whereas in the others there is a smooth trend through Eu. In the group above the Pyroxenite Marker there is a negative Eu anomaly, LREE enrichment and again a flat HREE trend. The transition group shows a diversity of Eu anomalies including both positive and negative ones. However, excluding Eu, the profiles are broadly similar with LREE enrichment and a flat HREE trend.

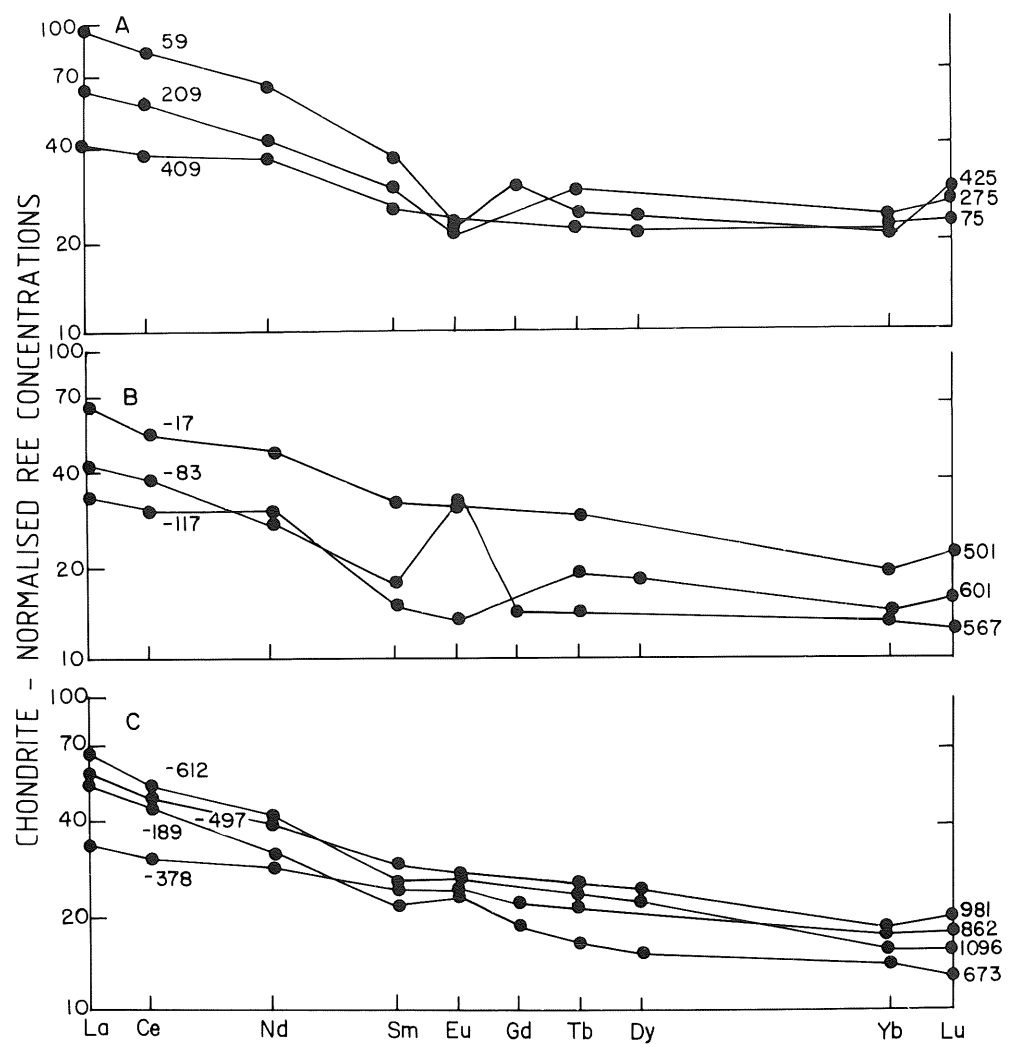


Figure 9: Calculated REE composition of the magma from which the analysed samples would have accumulated. See text for method of calculation. The samples are divided into the three different stratigraphic levels; A - above Pyroxenite Marker; B - zone of mixing below Pyroxenite Marker; C - below zone of mixing. Sample numbers as in Table 3; those on right of diagram refer to absolute depths; those on diagram refer to depths relative to the Pyroxenite Marker.

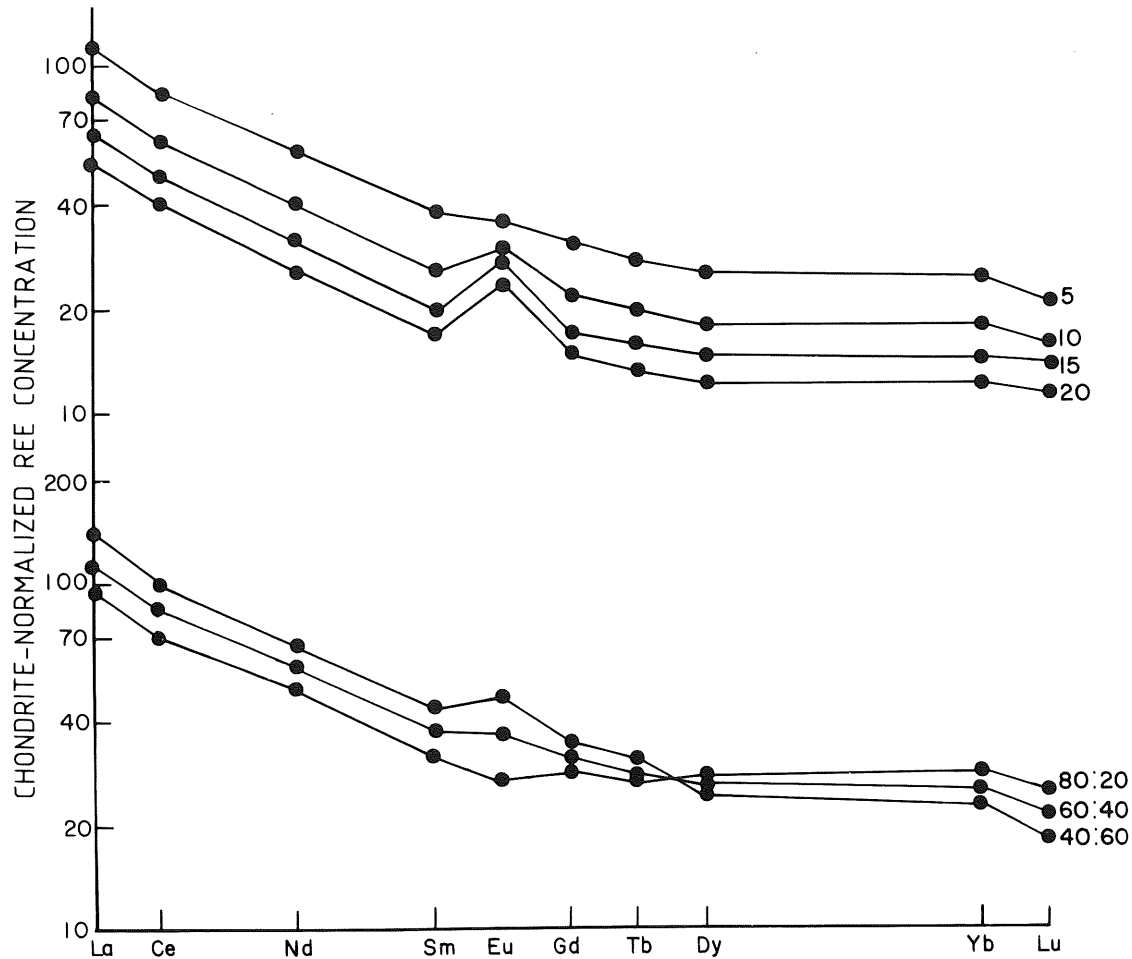


Figure 10: Plots of calculated liquid compositions for sample +189m, assuming different proportions (5, 10, 15, 20%) of intercumulus component (upper diagram), and different ratios (80:20; 60:40; 40:60) of plagioclase to pyroxene (lower diagram), based on equation in text and mineral partition coefficients in Table 5. These calculations illustrate that the calculated composition of the magma is not very sensitive to the proportion of minerals and intercumulus component in the cumulate.

The average REE patterns for the two groups are shown in Table 6 and Figure 11. The patterns are quite similar, although the following differences are noted. The $(La/Lu)-N$ ratio is slightly greater in the lower group than the upper, as is the ratio of the middle to heavy REE $(Sm + Gd)/(Yb + Lu)$. The lower group shows a positive Eu anomaly and the upper group a negative anomaly. The middle group, which is regarded as forming from the initial mixing of magmas, generally shows intermediate values.

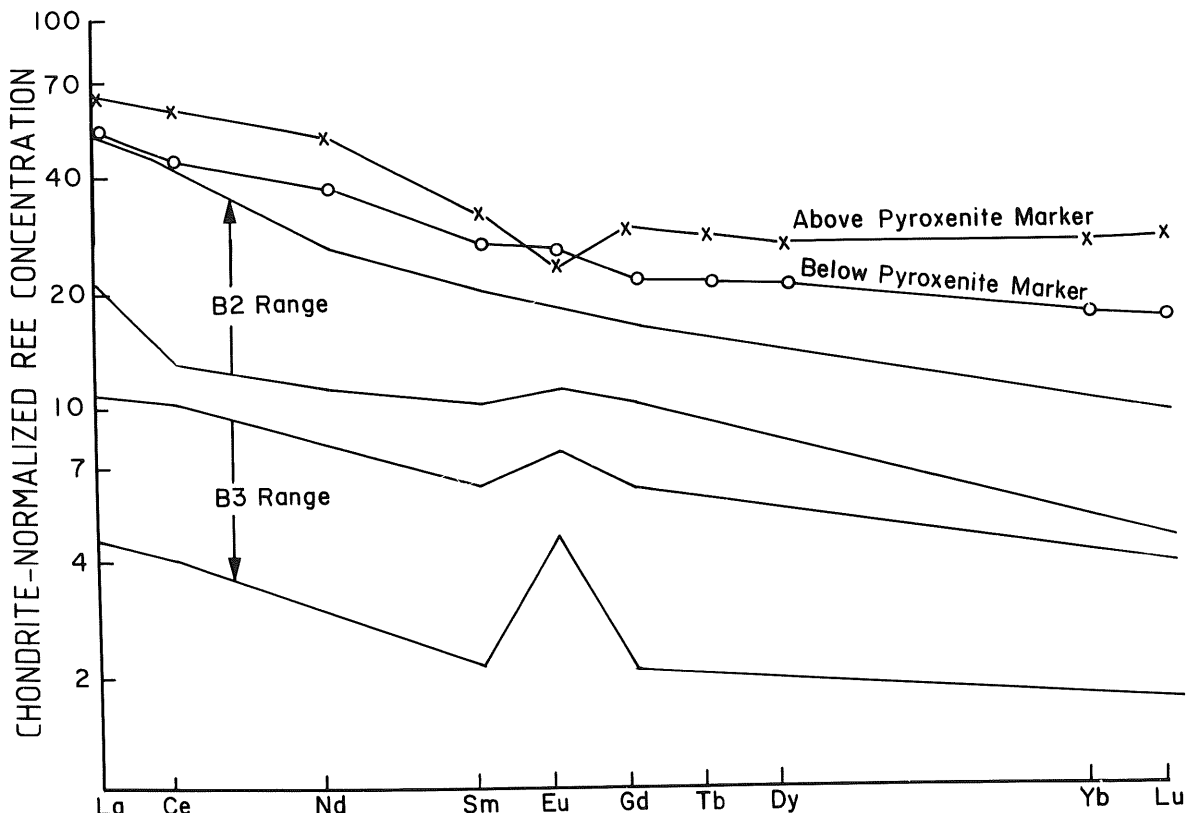


Figure 11: Plot of calculated chondrite-normalized REE compositions for the two magmas presumed to have produced the cumulate sequence below and above the Pyroxenite Marker (see Table 6). The postulated parental magmas to the Critical and Main Zones, B2 and B3 respectively (Harmer & Sharpe, 1985) are included for comparison. It seems very unlikely that the B3 (Main Zone) composition could have produced the cumulates observed in the present study because of the extremely low abundances of REE in the B3 magma.

For all these calculated magma compositions the partition coefficients for all phases have been assumed to be constant (see Table 5). Within all three groups the range of mineral compositions overlaps and so there will be no systematic differences in partition coefficients between

the groups due to differences in mineral composition. However, there is one difference which may be significant, namely the higher ferric iron content in the pyroxenes and plagioclase above the reversal (Fig. 4 and Table 1). This implies that the f_{O_2} was higher in the new magma. This would cause a decrease in the partition coefficient for Eu into plagioclase (Drake & Weill, 1975; Drake, 1975). Figure 7 shows that the magnitude of the Eu anomaly is not dependent upon the plagioclase composition or modal content, but upon the stratigraphic height of the sample, consistent with the increase in oxygen fugacity for the upper samples. If a partition coefficient of 0.20 is used instead of 0.35 into plagioclase for the upper group, the negative anomaly disappears in the calculated magma compositions. Such a change can readily be attributed to small changes in f_{O_2} . Consequently, the Eu anomalies indicated for the upper group in Table 6 may be an artifact of the constant partition coefficient used and may not be petrologically significant.

In Figure 9 the sample from -117 m shows a negative Eu anomaly in the calculated liquid composition. The pyroxene and plagioclase compositions of this sample indicate that they have formed from a mixed magma with a slightly higher f_{O_2} . Thus a lower partition coefficient for Eu might also be more appropriate in calculating the liquid for this sample.

These calculated REE contents for magmas forming the Main Zone can be compared with values obtained from fine-grained marginal rocks, and thought to be representative of magmas added at this level of the intrusion (Harmer & Sharpe, 1985). They are compared in Figure 11. There is reasonable agreement between the calculated Main Zone magma profiles and the B2 gabbronorite type of Harmer & Sharpe (1985). Approximately 30% gabbro fractionation of B2 magmas (represented by the cumulate interval from the Merensky Reef to the succession studied) would produce an even closer correspondence with the calculated REE pattern in Figure 11. However, these B2 magmas were regarded by Harmer & Sharpe (1985) as having been introduced as the Critical Zone was crystallizing. The magmas feeding the Main Zone (B3 type) in Harmer and Sharpe's model have radically different REE and trace element contents. They have Ce values of 4 - 10; Yb of 2-4; Zr = 23 ppm; and $P_{O_2}^{2/4} = 0.03$. Such values are comparable to those reported in Tables 2 and 4 for rocks which are demonstrably cumulates. These very low values in B3 compositions suggest dilution relative to the true liquid by cumulus phases.

Sharpe (1985) suggested that the Main Zone below the Pyroxenite Marker crystallized from a magma (B3 type) which intruded at the level of the Merensky Reef but did not mix with the resident magma. If this model is correct there should be reasonable agreement between the REE contents of B3 (inferred to be the parental magma) and the compositions determined here from the bulk rock compositions. It is evident from Figure 11 that there is no way in which such a B3 type magma could produce the gabbronorites with the chemistry of the Main Zone samples described here.

Other models for the formation of the lower Main Zone envisage magma addition and mixing. However, the composition of the supposed added magma varies from ultrabasic (Naldrett & Von Gruenewaldt, 1989), through mafic (Eales *et al.*, 1990) to anorthositic (Irvine & Sharpe, 1986); and in none of these interpretations is the REE content of the new magma indicated. Hence, it is impossible to test whether such magmas are appropriate in terms of their REE to produce the observed cumulates.

Magma Addition and Mixing at the Pyroxenite Marker

The break in mineral compositions and isotopic ratios leaves little doubt that there was addition of a distinct magma type during the crystallization of this sequence of rocks. It is therefore relevant to investigate the mechanism, geometry and dynamics of this process.

Up to -188 m crystallization was dominated by the gabbronorite assemblage with 60 % plagioclase. This would have lead to an increase in density in the differentiating liquid (Sparks *et al.*, 1980). The new magma crystallized more primitive mineral compositions and so would have been hotter than the residual magma. It was also lower in FeO and SiO₂, as shown previously; parameters which counteract each other in calculations of the liquid density (Bottinga & Weill, 1970). However, if the new magma had a lower density than the resident magma, it would have risen through and entrained the resident magma to form a metastable, hot, upper layer. Rapid heat loss upwards and downwards would have caused an increase in density in the new magma layer due to cooling and crystallization, and ultimately finger overturn or plunging of dense packets of magma plus crystals to the base of the magma column (Morse, 1986a). This is envisaged to have begun when the cumulate sequence had reached about -117 m. Thus at this level the plagioclase and pyroxene became enriched in An and En compared to those in the underlying sequence. If plagioclase at this level crystallized from the new (more oxidised) magma then the calculated Eu anomaly in the liquid (Fig. 9) can be explained. The plagioclase in the overlying sample at -83 m, shows a wide range of core compositions from An₀ to An₆₂⁷⁰ (Fig. 3). These compositions vary from close to those found in the underlying sample at -117 m formed from the new magma, to values approaching those found in the next sample downwards at -188 m formed from the resident magma. In other words, the plagioclase core compositions in the sample from -83 m are similar to those of plagioclase crystallized from both magmas. This could be interpreted in two ways:

- 1) the size of the plunging packets of magma plus crystals was very small and an inhomogeneous layer of these packets existed within a matrix of the resident magma; and
- 2) there was a suspension of pre-existing plagioclase (and pyroxene?) grains in the resident magma prior to the injection of the new magma, and that these accumulated together with the crystals formed from the new magma.

In the first model, it could be argued that the matrix of earlier magma, being in close proximity to packets of hotter new magma, would have become heated and would not have continued to crystallize. However, if nuclei were present in this earlier magma due to moderate degrees of undercooling (Morse 1986b; Jaupart & Brandeis, 1986; Mathison, 1987), growth of crystals could have continued even as the magma was being heated.

It does not seem possible to test these two hypotheses further. However, what is of major importance is that the mineral compositions of the sample at -83 m demonstrate that crystallization or accumulation of crystals was occurring simultaneously from two incompletely mixed magmas. The range of compositions of pyroxenes at any specific level is far more restricted than for the plagioclase (Fig. 3), presumably reflecting more rapid solid-state diffusion of Mg and Fe in pyroxene than CaAl and NaSi in plagioclase (Morse, 1984). Therefore, the feldspars preserve a more accurate record of the primary magmatic processes.

In contrast to the above hypothesis, the more restricted range of core compositions of plagioclase in samples above the Pyroxenite Marker points to crystallization from a magma which had become homogeneous and was not being chemically and thermally disturbed by further addition of magma, a conclusion supported by the uniformity of the initial Sr isotopic ratio from this horizon upwards (Kruger *et al.*, 1987). Thus effective mixing may have taken place close to the level of the Pyroxenite Marker.

Sharpe (1985) presented a radically different model for the origin of the Pyroxenite Marker and the inflection in Sr isotope composition. He suggested that, at the level of the Merensky Reef, there was addition of dense magma which underplated the resident magma and did not mix with it. This new, lower layer of magma partially crystallized to produce the Main Zone, below the Pyroxenite Marker, and then underwent dramatic mixing with the older, elevated magma to produce the Pyroxenite Marker and Sr isotopic break.

Thermal and density paradoxes exist for this model. The minerals below the Pyroxenite Marker are more differentiated than those above it. This demands that the underlying magma was cooler than the overlying layer. Almost all heat loss must be through the roof of a magma chamber (Marsh, 1989) and so this model therefore requires transport of heat against a thermal gradient. Furthermore, crystallization of a magnetite-free, plagioclase-dominated sequence would result in an increase in the density of the residual magma. Thus, if the overlying magma was less dense than the underlying magma at the time of its emplacement, the density contrast and gravitational stability should have been enhanced by the crystallization of the Main Zone cumulates. Therefore, the delayed mixing model of Sharpe (1985) is inconsistent with the predicted physical behaviour, and with the REE constraints discussed earlier.

Postcumulus Processes

A variety of postcumulus processes may contribute to the final solidification and composition of the rock. Models involving compaction (McKenzie, 1984; Hunter, 1987), infiltration metasomatism (Irvine, 1978) and compositional convection (Tait *et al.*, 1984) have been proposed to permit upward or downward percolation of interstitial liquid. Evidence for the vertical movement of residual liquids can be obtained from the Sr isotopic data. From Figure 8 and Kruger *et al.* (1987) it is apparent that the new magma had a lower initial Sr isotopic ratio than the resident magma.

The An composition of the cores of plagioclase grains in the sample at -117 m indicates that there was a large contribution from the new magma. However, the initial $^{87}\text{Sr}/^{86}\text{Sr}$ ratio (Table 4) is 0.7078 which is closer to the resident magma ratio of 0.7082 than the new magma ratio of 0.7063. As essentially all the Sr in the rock is present in the plagioclase, these two observations appear contradictory. This can be resolved by considering the downward plunging two-phase packets of plagioclase plus pyroxene and magma into the underlying resident magma. The cumulus plagioclase would record the lower initial $^{87}\text{Sr}/^{86}\text{Sr}$ ratio of the new magma, but would have been out of equilibrium with the resident magma. Different rates of re-equilibration in the plagioclase for Sr and An can be modelled quantitatively (Morse, 1984). He showed that the effective diffusion rate (D) for the $\text{CaAl} = \text{NaSi}$ exchange is in the order

of $10^{-20} \text{ cm}^2 \text{ sec}^{-1}$. In contrast, the diffusion rate for Sr through solid plagioclase is $10^{-13} \text{ cm}^2 \text{ sec}^{-1}$ (Hofmann & Hart, 1978). Morse considered subsolidus diffusion, whereas here the interaction would have occurred above the solidus. Hence, temperatures would be higher, but the time available less than in Morse's calculations. However, allowing 3×10^4 years for the interval from accumulation to solidification of the rock, homogenisation of the Sr isotopes in plagioclase could have occurred over a distance of 0.3cm, even though the An content would not have changed significantly during this period. This distance is comparable to the size of plagioclase grains.

If the resident magma percolated, or was displaced, upwards by the plunging packages, and reacted with the plagioclase of the new magma, the extent of resetting of the isotopic ratios in the bulk rock would have decreased with increasing height. Progressively higher samples would show smaller amounts of resetting and have ratios which gradually approached that of the cumulates from the partially mixed magma, as is observed up to -17 m (Fig. 8). A schematic diagram depicting these effects is shown in Figure 12.

From the Pyroxenite Marker to +59 m the isotopic ratio increases. The samples from a height of +59 m to the top of the intrusion (about 2km) define an isochron with an initial $^{87}\text{Sr}/^{86}\text{Sr}$ ratio of 0.7073 ± 1 (Kruger *et al.*, 1987). The magma from which these rocks formed was therefore isotopically homogeneous. In contrast, the compositions of samples from -117 to -17 m indicate that they formed from an inhomogeneous magma body which was dominated by the new magma and had an isotopic ratio less than 0.7073. If the interstitial liquid to this sequence filtered upwards it would lower the isotopic ratio in the overlying cumulates as is observed in the trend from 0 to +59 m (Figs. 8 and 12).

The Pyroxenite Marker has an initial isotopic ratio which is slightly lower than expected from the smooth trend on Figure 8. As the rock contains much less plagioclase and hence less Sr than other samples, the upward-percolating liquid would have produced a larger shift in the ratio (to lower values) compared to adjacent plagioclase-rich samples.

The new magma crystallized pyroxenes enriched in Al, Ti, and Cr, but the upward percolation of magma would also have affected these elements as well as the Mg/(Mg+Fe) ratio. The lowermost samples above the level of magma addition; i.e. from -117 m; would have experienced a significant degree of resetting by this magma, producing the break in compositions recognised in Figure 5 above -117 m.

Pyroxenite Marker

The Pyroxenite Marker in the eastern Bushveld Complex has been used as a lithological boundary in the subdivision of the Bushveld Complex (Von Gruenewaldt, 1973). The same horizon has been recognised in this study at 484 m in the BK2 borehole from the western Bushveld. However, unlike the eastern Bushveld, inverted pigeonite disappears 100 m below the Pyroxenite Marker (Fig.2), in the western Bushveld. Furthermore, the major reversal in mineral compositions is initiated at -117 m (Figs. 3 to 5). In fact, the Pyroxenite Marker occurs close to the top of the zone of magma addition and mineralogical inhomogeneity. It is distinctive in being devoid of cumulus plagioclase, and so is a useful marker horizon. However, it marks the culmination of a prolonged mixing event, not its initiation.

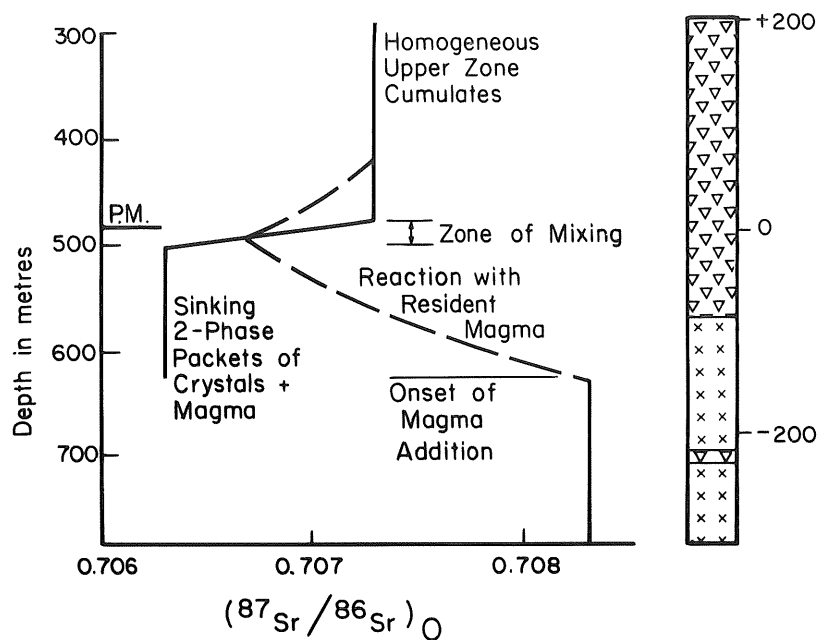


Figure 12: Model showing the potential changes in initial $^{87}\text{Sr}/^{86}\text{Sr}$ isotope ratio due to magma addition. The solid line shows the isotopic composition of the cumulus minerals which, up to 150m below the Pyroxenite Marker, is the same as the bulk rock composition. At this level magma was added but stratified above the base of the magma column, cooled, and crystallized. Packets of crystals plus magma with a lower isotopic ratio then sank into the underlying magma. Reaction of these crystals and mixing of the new magma with the resident magma produced the steadily decreasing hybrid isotopic ratios seen from -150m up to the Pyroxenite Marker, shown as the dashed line. Above the Pyroxenite Marker, the cumulus minerals have a constant isotopic ratio due to thorough mixing (see Kruger *et al.*, 1987). However, upward infiltration from the underlying crystal mush caused a partial resetting to lower values of the bulk rock isotopic ratio as indicated by the dashed line. The isotopic profile generated by this mixing model can be compared with the observed ratios plotted in Figure 8. The slight irregularities in the part of the curve in Figure 8 where reaction between resident magma and sinking cumulus crystals occurred is due to the variations in the proportion of plagioclase to pyroxene in these rocks (see text for discussion).

SUMMARY

Several petrological aspects relating to a major addition of magma in the Main Zone of the Bushveld Complex are presented. The volume of magma added was comparable to that already in the reservoir. Its initial $^{87}\text{Sr}/^{86}\text{Sr}$ ratio was 0.7063, considerably less than that of the resident magma. The pyroxenes which formed from the new magma contained higher TiO_2 , Al_2O_3 , Fe_2O_3 and Na_2O at the same $\text{Mg}/(\text{Mg}+\text{Fe})$ ratio than those from the resident magma suggesting that the new magma had lower silica and higher $f\text{O}_2$. Modelling of the REE abundances in the two magmas indicated that both had slight LREE enrichment and a flat HREE profile. These calculated compositions do not match some of the postulated magma compositions claimed to be injected during the formation of the Main Zone. The added magma had lower density than the resident magma and so rose and entrained resident magma. Rapid loss of heat resulted in the raining of packets of magma plus crystals to the floor of the chamber. Sr isotope exchange between plagioclase from the new magma and the residual magma caused resetting of the bulk isotopic ratio, but the slow re-equilibration between the An and Ab components of the plagioclase permitted preservation of the primary plagioclase compositions. The Pyroxenite Marker occurs close to the top of the cumulate succession which records this mixing event. The onset of magma introduction may be recognised by the disappearance of inverted pigeonite, together with the initiation of a reversal in mineral compositions and a secular change in initial $^{87}\text{Sr}/^{86}\text{Sr}$ ratio.

ACKNOWLEDGEMENTS

This project would not have been possible without the access to the bore core drilled by the Geological Survey of South Africa, whose support is greatly appreciated. Dr. F. Walraven and Mr. F. Moen of the Geological Survey provided invaluable assistance in sampling and other information, and permission to publish by the Chief Director, Dr. C. Frick, is gratefully acknowledged. The writers are indebted to Jean-Guy Schilling and Brian McCully for assistance with the neutron activation analyses, and to Haraldur Sigurdsson for providing electron microprobe facilities; all at the University of Rhode Island. Reviews by H.V. Eales, J.R. Wilson, J. Wadsworth and J.R. McIver helped to clarify the authors' ideas and the manuscript. R.G.C. and F.J.K. are supported by the Foundation for Research Development (South Africa).

REFERENCES

- ATKINS, F.B., 1969. Pyroxenes of the Bushveld Intrusion, South Africa. J. Petrology, 10, 222-249.
- BOTTINGA, Y., & WEILL, D.F., 1970. Densities of liquid silicate systems calculated from partial molar volumes of oxide components. Amer. J. Sci., 269, 169-182.
- CAMPBELL, I.H., & TURNER, J.S., 1989. Fountains in magma chambers. J. Petrology 30, 885-924.

- CAWTHORN, R.G., 1983. Magma addition and possible decoupling of major- and trace-element behaviour in the Bushveld Complex, South Africa. Chem. Geol., 39, 335-345.
- _____, & COLLERSON, K.D., 1974. The recalculation of pyroxene end-member parameters and the estimation of ferrous and ferric iron contents from electron microprobe analyses. Amer. Mineral. 59, 1203-1208.
- _____, & WALSH, K.L., 1988. The use of phosphorus contents in yielding estimates of the proportion of trapped liquid in cumulates of the Upper Zone of the Bushveld Complex. Mineral. Mag., 52, 81-89.
- _____, DAVIES G., CLUBLEY-ARMSTRONG, A., & McCARTHY, T.S., 1981. Sills associated with the Bushveld Complex, South Africa: an estimate of the parental magma composition. Lithos, 14, 1-15.
- COERTZE, F.J., 1970. The geology of the western part of the Bushveld Igneous Complex. Geol. Soc. S. Afr. Spec. Publ., 1, 5-22.
- COOMBS, D.S., 1963. Trends and affinities of basaltic magmas and pyroxenes as illustrated on the diopside-olivine-silica diagram. Mineral. Soc. Am. Spec. Paper, 1, 227-250.
- CZAMANSKE, G.K., & SCHEIDLE, D.L., 1985. Characteristics of the banded-series anorthosites. Montana Bureau Mines and Geology, Spec. Publ., 92, 334-345.
- DAVIES, G., & CAWTHORN, R.G., 1984. Mineralogical data on multiple intrusion in the Rustenburg Layered Suite of the Bushveld Complex. Mineral. Mag., 48, 469-480.
- _____, & TREDOUX, M., 1985. The platinum-group element and gold contents of the marginal rocks of the Bushveld Complex. Econ. Geol., 80, 838-848.
- DRAKE, M.J., 1975. The oxidation state of europium as an indicator of oxygen fugacity. Geochim. Cosmochim. Acta, 39, 55-64.
- _____, & WEILL, D.F., 1975. Partition of Sr, Ba, Ca, Y, Eu, Eu* and other REE between plagioclase feldspar and magmatic liquid: an experimental study. Geochim. Cosmochim. Acta, 39, 689-712.
- EALES, H.V., DE KLERK, W.J., BUTCHER, A.R., & KRUGER, F.J., 1990. The cyclic unit below the UG1 chromitite (UG1FW unit) at RPM Union Section Platinum Mine - Rosetta stone of the upper Critical Zone? Mineral. Mag., 54, 23-43.
- HAMILTON, P.J., 1977. Sr isotope and trace element studies of the Great Dyke and Bushveld mafic phase and their relation to early Proterozoic magma genesis in Southern Africa. J. Petrology, 18, 24-52.

- HARMER, R.E., & SHARPE, M.R., 1985. Field relations and strontium isotope systematics of the marginal rocks of the eastern Bushveld Complex. Econ. Geol., 80, 813-837.
- HENDERSON, P., 1968. The distribution of phosphorus in the early and middle stages of fractionation of some basic layered intrusions. Geochim. Cosmochim. Act., 32, 897-911.
- _____, 1975. Geochemical indicator of the efficiency of fractionation of the Skaergaard Intrusion, East Greenland. Mineral. Mag., 40, 285-291.
- HOFMANN, A.W., & HART, S.R., 1978. An assessment of local and regional isotopic equilibrium in the mantle. Earth Planet. Sci. Lett., 38, 44-62.
- HUNTER, R.H., 1987. Textural equilibrium in layered igneous rocks, in Parsons, I. (Ed.) Origins of Igneous Layering. Reidel Publishing Co., 573-503.
- IRVINE, T.N., 1978. Infiltration metasomatism, adcumulus growth, and secondary differentiation in the Muskox intrusion. Carnegie Inst. Washington, Yrbk., 77, 743-751.
- _____, 1982. Terminology for layered intrusions. J. Petrology, 23, 127-162.
- _____, KEITH, D.W., & TODD, S.G., 1983. The J-M platinum-palladium reef of the Stillwater Complex, Montana. II. Origin by double-diffusive convective magma mixing and implications for the Bushveld Complex. Econ. Geol., 78, 1287-1334.
- _____, & SHARPE, M.R., 1986. Magma mixing and the origin of stratiform oxide ore zones in the Bushveld and Stillwater Complexes, in Gallagher, M.J., Ixer, R.A., Neary, C.R., & Pritchard, H.M. (Eds.), Metallogeny of Basic and Ultrabasic Rocks, Institution of Mining Metallurgy, London, 183-198.
- IRVING, A.J., 1978. A review of experimental studies of crystal/liquid trace element partitioning. Geochim. Cosmochim. Acta, 42, 743-770.
- JAUPART, C., & BRANDEIS, G., 1986. The stagnant bottom layer of convecting magma chambers. Earth Planet. Sci. Lett., 80, 183-199.
- KRUGER, F.J., CAWTHORN, R.G., & WALSH, K.L., 1987. Strontium isotope evidence against magma addition in the Upper Zone of the Bushveld Complex. Earth Planet. Sci. Lett., 84, 51-58.
- LINDSLEY, D.H., 1983. Pyroxene thermometry. Amer. Mineral., 65, 477-493.
- MARSH, B.D., 1989. On convective style and vigor in sheet-like magma chambers. J. Petrology, 30, 479-530.

- MATHISON, C.I., 1987. Pyroxene oikocrysts in troctolitic cumulates - evidence for supercooled crystallization and postcumulus modification. Contrib. Mineral. Petrol., 97, 228-236.
- McKENZIE, D.P., 1984. The generation and compaction of partially molten rock. J. Petrology, 25, 713-765.
- MOLYNEUX, T.G., 1974. A geological investigation of the Bushveld Complex in Sekhukuneland and part of the Steelpoort valley. Trans. Geol. Soc. S. Afr., 77, 329-338.
- MORSE, S.A., 1984. Cation diffusion in plagioclase feldspar. Science, 225, 504-505.
- 1986a. Thermal structure of crystallizing magma with two-phase convection. Geol. Mag., 123, 205-214.
- 1986b. Convection in aid of adcumulus growth. J. Petrology, 27, 1183-1214.
- NALDRETT, A.J. & VON GRUENEWALDT, G., 1989. The association of PGE with chromitite in layered intrusions and ophiolite complexes. Econ. Geol., 84, 180-187.
- SCHILLING, J.G., & RIDLEY, W.I., 1975. Volcanic rocks from DSDP Leg 29: Petrography and rare earth abundances. Initial Rep. Deep Sea Drilling Project, 29, 1103-1197.
- SHARPE, M.R., 1981. The chronology of magma influxes to the eastern compartment of the Bushveld Complex as exemplified by its marginal border groups. J. Geol. Soc. London, 138, 307-326.
- 1985. Strontium isotope evidence for preserved density stratification in the main zone of the Bushveld Complex, South Africa. Nature, 316, 119-126.
- SPARKS, R.S.J., HUPPERT, H.E., & TURNER, J.S., 1984. The fluid dynamics of evolving magma chambers. Phil. Trans. Roy. Soc. London, A310, 511-534.
- , MEYER, P., & SIGURDSSON, H., 1980 Density variation amongst mid-ocean ridge basalts: implications for magma mixing and the scarcity of primitive lavas. Earth Planet. Sci. Lett., 46, 419-430.
- TAIT, S.R., HUPPERT, H.E., & SPARKS, R.S.J., 1984. The role of compositional convection in the formation of adcumulate rocks. Lithos, 17, 139-146.
- TURNER, J.S., & CAMPBELL, I.H., 1986. Convection and mixing in magma chambers. Earth Sci. Rev., 23, 255-352.
- VON GRUENEWALDT, G., 1973. The Main and Upper Zone of the Bushveld Complex in the Roossenekal area, eastern Transvaal. Trans. Geol. Soc. S. Afr., 76, 207-227.

- WAGER, L.R., & BROWN, G.M., 1968. Layered igneous rocks. Oliver and Boyd, Edinburgh, 588pp.
- —, & WADSWORTH, W.J., 1960. Types of igneous cumulates. J. Petrology, 1, 73-85.
- WALRAVEN, F., & WOLMARANS, L.G., 1979. Stratigraphy of the upper part of the Rustenburg Layered Suite, Bushveld Complex, in western Transvaal. Annals Geol. Surv. S. Afr., 13, 109-114.
- ARMSTRONG, R.A., & KRUGER, F.J., 1990. A chronostratigraphic framework for the north-central Kaapvaal craton, the Bushveld Complex and Vredefort structure. Tectonophysics, 171, 23-48.
- WATSON, E.B., & GREEN, T.H., 1981. Apatite/liquid partition coefficients for the rare earth elements and strontium. Earth Planet. Sci. Lett., 56, 405-421.

____oo____